

# Radiation behaviour of mm-wave on-wafer probes in H-band and the influence on antenna measurements

Joachim Hebel, <sup>✉</sup> Thomas Zwick, and Akanksha Bhutani

*Institute of Radio Frequency Engineering and Electronics, Karlsruhe Institute of Technology, Karlsruhe, Germany*

<sup>✉</sup> E-mail: joachim.hebel@kit.edu

This letter presents a comprehensive analysis of the radiation behaviour exhibited by nine distinct on-wafer radio-frequency (RF) probes used for device characterization in the mm-wave bands of integrated circuits and antennas. The tested probes are sourced from two different manufacturers and feature various probe pitches. All probes are intended for use with the WR-3.4 waveguide band ranging from 220 to 330 GHz. To the best of the authors' knowledge, such a detailed examination of RF probes operating in this band with respect to their radiation behaviour has not been demonstrated before.

**Introduction:** With an increasing interest in mmWave frequency bands, test and measurement tasks have become more challenging and frequent. Essential in measuring these devices are radio-frequency (RF) probes contacting devices to avoid complicated and troublesome interconnect solutions to the nearest waveguide band [1]. However, these probes' influence on the measurement is a critical aspect [2, 3] with previous works investigating the probe influence on radiation measurements at frequencies below 67 GHz [4–7]. One aspect that still needs to be evaluated is the radiation of probes operating at mm-wave frequencies. This letter investigates the probe radiation behaviour, especially in the H-band.

This work focuses on two styles of probes operating in the H-band using the WR-3.4 waveguide. These are *PicoProbe 325B* by GGB and *Infinity Waveguide i325* by FormFactor. The latter one is offered with different pin pitch options, of which a pitch of 100 and 50  $\mu\text{m}$  are tested. Table 1 lists the tested probes within this work, their pitch, production year, and the designator by which they are referenced in this letter.

**Probe construction:** Both probes tested here are described in [8]. The *FormFactor Infinity Waveguide* probes have a transition from a rectangular waveguide to a micro-coax. This coax is brought out to the probe tip and is part of the mechanical construction. A micrograph is shown in Figure 1a. The end of the coax is ground down to a specific shape, and a small printed circuit board (PCB) out of copper and polyamide is attached. The PCB connects the centre conductor of the coax to the probe tips on the PCB. The tip is then secured with the epoxy glue visible in Figure 1a.

The *GGB 325B* probe consists of a rectangular waveguide to coplanar waveguide (CPW) transition. This coplanar waveguide is brought out and tapered to form the ground-signal-ground (GSG) probe tip contacting the substrate. The length of the exposed CPW is less than 250  $\mu\text{m}$ .

Table 1. Used probes and their designation

Designation	Type	Pitch	Year
C1 50um	Micro-Coax	50 $\mu\text{m}$	2021
C2 50um	Micro-Coax	50 $\mu\text{m}$	2021
C3 50um	Micro-Coax	50 $\mu\text{m}$	2023
C4 100um	Micro-Coax	100 $\mu\text{m}$	2022
C5 100um	Micro-Coax	100 $\mu\text{m}$	2022
C6 100um	Micro-Coax	100 $\mu\text{m}$	2023
ACP 1	ACP	80 $\mu\text{m}$	2016
ACP 2	ACP	80 $\mu\text{m}$	2014
ACP 3	ACP	80 $\mu\text{m}$	2014

Abbreviation: ACP, air-coplanar.

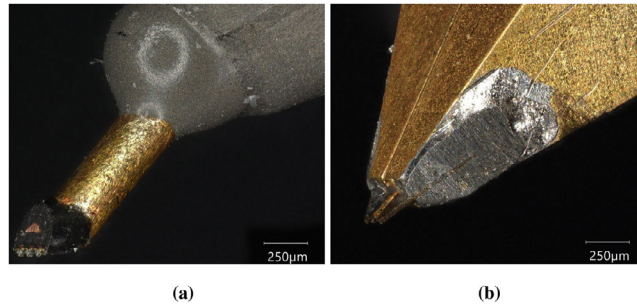


Fig. 1 Micrograph of the used RF probes. (a) The coax probe with the micro coax going to the probe tip. (b) The air-coplanar probe with the coplanar waveguide forming the probe tip. RF, radio-frequency frequency

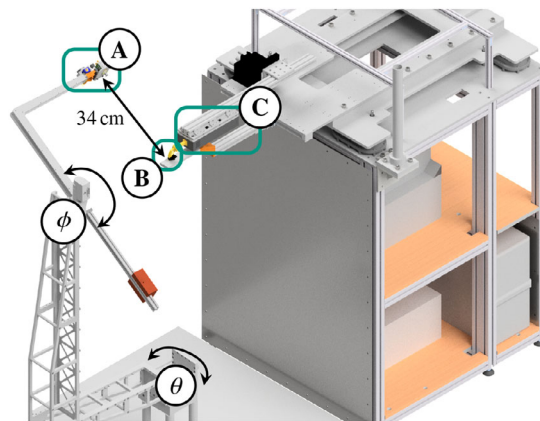


Fig. 2 Antenna measurement setup used to characterize the probe radiation. A marks the receiver that is rotated around the two axis  $\theta$  and  $\phi$ . In the centre of the rotation is the antenna under test, denoted B. The transmitter is marked C

A micrograph of the probe is shown in Figure 1b. As the contacts are suspended in air the type is referenced as air-coplanar (ACP).

**Measurement setup:** The radiation of the probes is measured using a free space antenna measurement setup presented in [9] and shown in Figure 2. As a receiver, a VDI *MixAMC-I WR-3.4* active fundamental mixer is used together with a *MiWave* standard gain horn antenna. The transmitter side is a VDI *VNAX WR-3.4* transmit/receive module connected to a *Keysight N5247B* VNA and *N5261A* head controller. The distance between the antenna under test to the receiver is 34 cm. The antenna measurement station is made of aluminium, plastic and covered in absorber material to reduce reflections. The probes are measured for two scenarios: one is open in the air, and the other is over an aluminium surface present in specific antenna measurement scenarios and during one-port calibration on an impedance standard substrate (ISS). The holder for the ISS visible in Figure 2 is removed for the probe in air measurement to prevent reflections. The VNA is calibrated to the waveguide flange of the transmit/receive module using short, quarter wavelength short, and load calibration standards. The antenna gain is calibrated using a standard gain horn and known antenna calibration. The measurement plane with  $\theta$  equal to  $0^\circ$  is denoted *E*-plane while the plane with  $\theta = 90^\circ$  is denoted *H*-plane. Due to the measurement setup, only a  $\phi$  angle up to  $210^\circ$  and down to  $-30^\circ$  in the *H*-plane is measurable. The measurements do not consider the insertion loss of the probes through the connecting waveguide and transitions. Including the probe loss will increase the radiated power but will not yield further insights.

**Measurement:** First, the radiation in the *E*-plane is measured for all nine probes free in the air. The results are shown in Figure 3 for the six coax probes and in Figure 4 for the three ACP probes. Clearly, the measured ACP probes radiate a lot less than the coax probes. Also, the radiation is heavily probe-dependent and differs by up to 12 dB. There is no correlation to the probe pitch or the manufacturing year, as evident from Figure 3.

Figures 5 and 6 show the measurements for the *H*-plane. Here, the reflection on the probe body is visible. The upper hemisphere from  $-90^\circ$

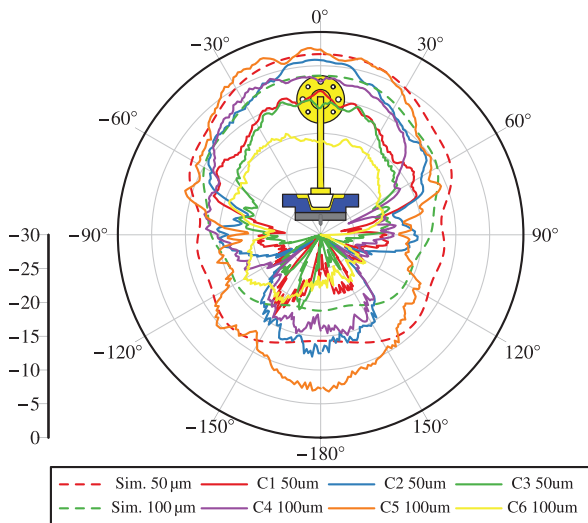


**Fig. 3** E-plane radiation measurement of the tested coax probes open in the air. In dashed lines are the simulation results for 50 and 100  $\mu\text{m}$  pitch

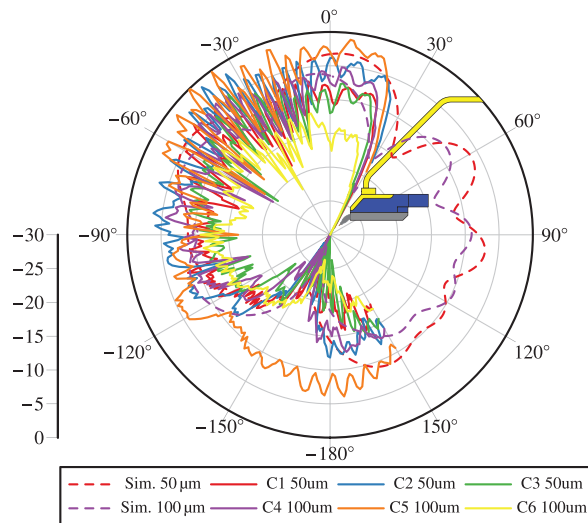


**Fig. 5** H-plane radiation measurement of the tested coax probes open in the air. In dashed lines are the simulation results for 50 and 100  $\mu\text{m}$  pitch

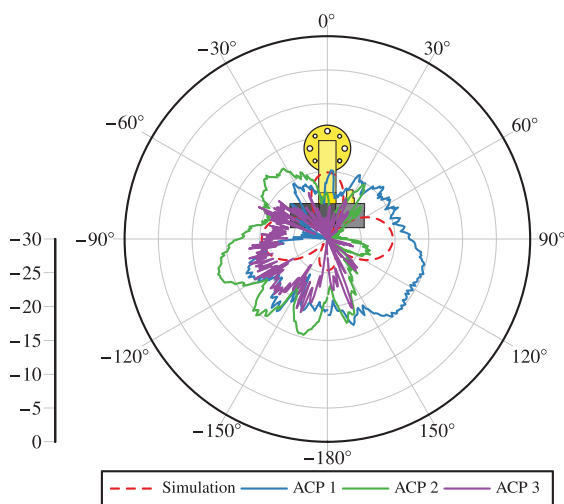


**Fig. 4** Measured E-plane radiation behaviour of the tested air-coplanar probes open in air. In dashed lines are the simulations

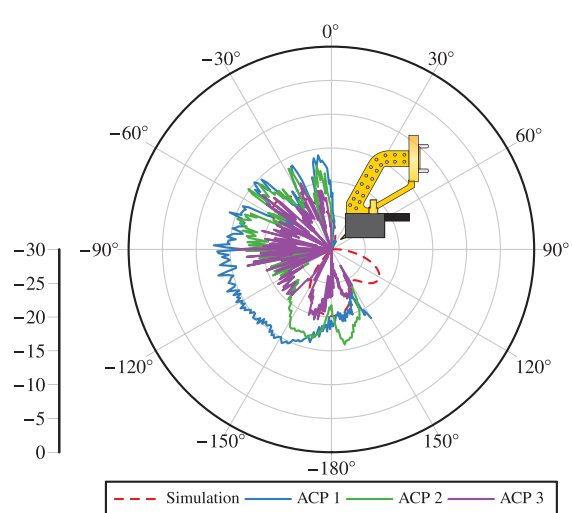


**Fig. 6** Measured H-plane radiation behaviour of the tested air-coplanar probes open in air. In dashed lines are the simulations

to  $0^\circ$  sees very strong interference. Another noteworthy aspect is that the coax probes tend to radiate upwards to  $0^\circ$  while the ACP probes tend to radiate in the direction of the CPW line. The probe shadow is another interesting aspect comparing Figures 5 and 6. While the coax probes allow radiation up to a  $\phi$  angle of around  $25^\circ$ , the ACP probes shadow at around  $0^\circ$ .

Also plotted in Figures 3 to 6 are the simulations for the three probe types used. The simulation results are obtained by creating geometric accurate model in *CST Studio Suite* and simulating these structures free in air [8]. Considering the E-plane, the simulations hint at stronger radiation for the 50  $\mu\text{m}$  pitch probes compared to the 100  $\mu\text{m}$  probes, which is not visible in the measurements. However, it correctly predicts the reduced radiation in the lower half, not the radiation zeros at  $\pm 120^\circ$  visible in all measurements except for C5 100 $\mu\text{m}$ . For the ACP probes, the simulation predicts more considerable radiation in the  $0^\circ$  direction, which is not present in the measurements. The more dominant radiation to the lower half is absent in the simulations. Considering the H-planes, both simulations for the coax probes capture the radiation zero at  $160^\circ$ , but not the reflection on the probe body, as it is not part of the simulation model.

Further, looking at the radiation at boresight, that is,  $\phi = 0^\circ$ , over frequency for both cases in Figure 7a,b shows that the radiation for all coax probes increases with frequency, reaching levels of close or above 0 dBi. This is also true for the simulations shown in dashed lines. The ACP probe stays relatively constant at  $-20$  dBi, while the simulation would also indicate an increase in radiated power with frequency.

The measurement with the probe free in the air is one extreme case that arguably is not realistic, as during measurements, a device under

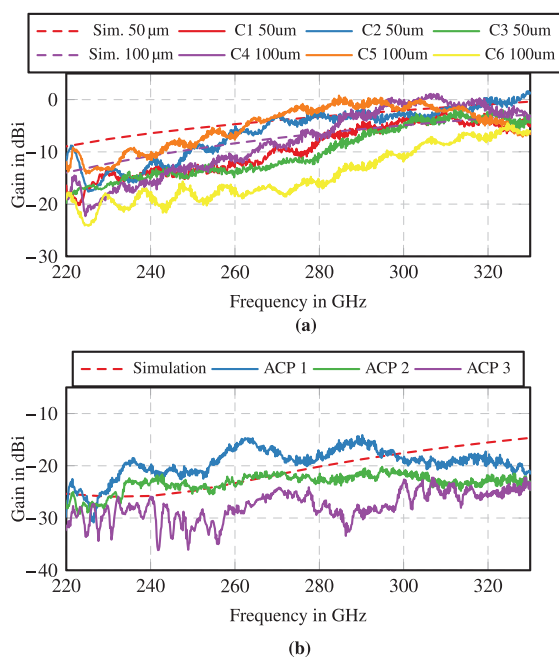


**Fig. 7** Measured radiation at boresight over frequency. The dashed lines show the simulation results for the 50 and 100  $\mu\text{m}$  coax probes in (a) and for the air-coplanar probe in (b)

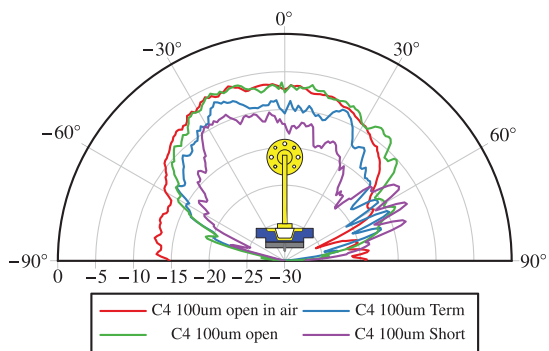


**Fig. 8** Measured pattern with C4 100um contacting open, short and load standards on an impedance standard substrate at 280 GHz

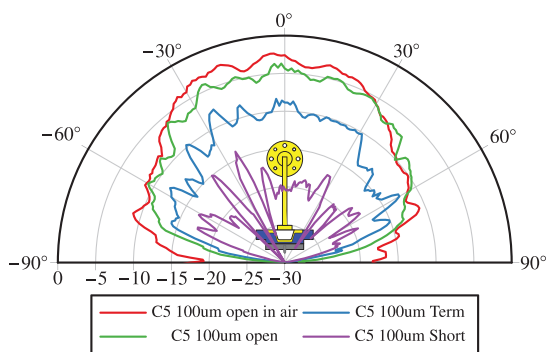


**Fig. 9** Measured pattern with C5 100um contacting open, short and load standards on an impedance standard substrate at 280 GHz

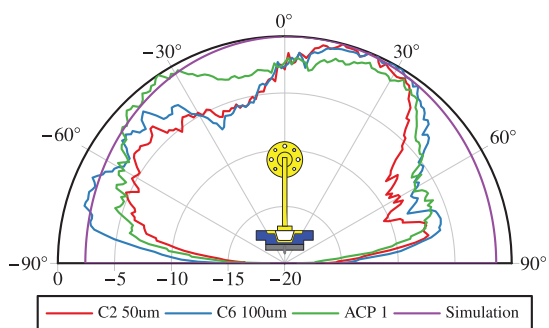


**Fig. 10** Normalized E plane field pattern at 250 GHz for the same bow-tie antenna measured with the ACP 1 probe and the C2 50um and C6 100um coax probes together with the simulation of the antenna itself. Clearly, the coax probe radiation influences the pattern, with a significant lobe pointing to the side

test (DUT) is connected. Ideally, the DUT presents an impedance close to a match. To test how the probes radiate when contacting a DUT, the short, open and load standard of an impedance standard substrate (ISS) are contacted. Figures 8 and 9 show this measurement for two coax probes, as they have the highest radiated power. The apparent result is that contacting the termination on the ISS does not reduce the power as much as contacting the short, even though it should dissipate more power. This hints at possible root issues in the probe construction where RF currents can travel along exposed metal. Another aspect is that radiated energy can vary quite significantly depending on the match of the DUT and will have a varying influence depending on the DUT.

**Influences on measurements:** A planar dipole antenna is measured with two of the coax probes and one ACP probe to evaluate the influence of the observed radiation in a realistic measurement. Figure 10 shows the measured and simulated pattern in the E-plane. The radiation of the used C2 50um probe is enough to cause a detrimental change in the pattern with a strong lobe pointing to 25°, an artifact of the slight offset of the probe from the used dipole antenna. This pattern is also visible using the theoretically better C6 100um probe, although the ratio of the side lobes becomes smaller. The measurement using the ACP probe does

not show this artifact. However, the influence of the probe body on the boresight direction is visible with a reduction of the pattern compared to the simulated one, which is expected from Figure 6.

**Conclusion:** Two different construction styles for waveguide probes operating in the H-band for on-wafer characterization are measured for their radiation behaviour. These measurements show that one style of probe using a micro-coax to feed RF pins has significant radiation that can exceed 0 dBi in certain circumstances. This radiation is, however, very dependent on the actual probe, as different samples within the same family differ pretty significantly from each other. Antenna measurements prove that this radiation is significant enough to invalidate antenna measurements. The measured style of ACP probes is significantly better in terms of radiation. However, antenna measurements suffer from the probe construction and reflections on the probe body. Simulation models of the probes can predict some of the radiation but lack some effects.

**Author contributions:** **Joachim Hebler:** Formal analysis; investigation; methodology; writing—original draft; writing—review and editing. **Thomas Zwick:** Conceptualization; funding acquisition; project administration; supervision; validation; writing—review and editing. **Akanksha Bhutani:** Conceptualization; methodology; project administration; supervision; validation; writing—review and editing.

**Acknowledgements:** This work was supported by the German Research Foundation (DFG) in the framework of the project ADAMIS (project number 394221495). This work is supported in part by BMBF within the funding for the programme Forschungslabore Mikroelektronik Deutschland (ForLab) under the reference 16ES0948.

**Conflict of interest statement:** The authors declare no conflicts of interest.

**Data availability statement:** Data available on request from the authors.

© 2024 The Authors. *Electronics Letters* published by John Wiley & Sons Ltd on behalf of The Institution of Engineering and Technology.

This is an open access article under the terms of the Creative Commons Attribution License, which permits use, distribution and reproduction in any medium, provided the original work is properly cited.

Received: 20 December 2023 Accepted: 28 January 2024

doi: 10.1049/ell2.13116

## References

- Zwick, T., et al.: Probe based mmw antenna measurement setup. *IEEE Antennas Propag. Soc. Symp.* **2004**(1), 747–750 (2004)
- Probst, T., et al.: 110 GHz on-wafer measurement comparison on alumina substrate. In: Proceedings of the 2017 90th ARFTG Microwave Measurement Symposium (ARFTG), vol. **1**, pp. 1–4. IEEE, Piscataway, NJ (2017)
- Phung, G.N., Arz, U.: Parasitic probe effects in measurements of coplanar waveguides with narrow ground width. In: Proceedings of the 2020 IEEE 24th Workshop on Signal and Power Integrity (SPI), vol. **1**, pp. 1–4. IEEE, Piscataway, NJ (2020)
- Yang, Q.H., et al.: Impact of on-wafer probe on the radiation measurement of a filtering antenna-in-package. In: Proceedings of the 2021 International Conference on Microwave and Millimeter Wave Technology (ICMMT), vol. **1**, pp. 1–3. IEEE, Piscataway, NJ (2021)
- Zheng, Z., Zhang, Y.P.: A study on the radiation characteristics of microelectronic probes. *IEEE Open J. Antennas Propag.* **3**, 4–11 (2022). doi:https://doi.org/10.1109/OJAP.2021.3131239
- Liu, Q., et al.: Influence of on-wafer probes in mm-wave antenna measurements. In: Proceedings of the 12th European Conference on Antennas and Propagation (EuCAP 2018), vol. **1**, pp. 1–5. IEEE, Piscataway, NJ (2018)
- Reniers, A.C.F., et al.: The influence of the probe connection on mm-wave antenna measurements. *IEEE Trans. Antennas Propag.* **63**(9), 3819–3825 (2015). https://doi.org/10.1109/TAP.2015.2452941
- Müller, D.: *RF Probe-Induced On-Wafer Measurement Errors in the Millimeter-Wave Frequency Range*. KIT Scientific Publishing, Karlsruhe (2018)
- Beer, S., Zwick, T.: Probe based radiation pattern measurements for highly integrated millimeter-wave antennas. In: Proceedings of the Fourth European Conference on Antennas and Propagation, vol. **1**, pp. 1–5. IEEE, Piscataway, NJ (2010)